A R C H I V E O F M E C H A N I C A L E N G I N E E R I N G

Volume 68 2021 Number 4

DOI: 10.24425/ame.2021.138397

Key words: damage detection, beam, modal parameters, mechanical failure, cracks, finite element model

Reza Taghipour[1], Mina Roodgar Nashta[1], Mohsen Bozorgnasab[1], Hessam Mirgolbabaei [2]

A new index for damage identification in beam structures based on modal parameters

The structural damages can lead to structural failure if they are not identified at early stages. Different methods for detecting and locating the damages in structures have been always appealing to designers in the field. Due to direct relation between the stiffness, natural frequency, and mode shapes in the structure, the modal parameters could be used for the purpose of detecting and locating the damages in structures. In the current study, a new damage indicator named "DLI" is proposed, using the mode shapes and their derivatives. A finite element model of a beam is used, and the numerical model is validated against experimental data. The proposed index is investigated for two beams with different support conditions and the results are compared with those of two well-known indices – MSEBI and CDF. To show the capability and accuracy of the proposed index, the damages with low severity at various locations of the structures containing the elements near the supports were investigated. The results under noisy conditions are investigated by considering 3% and 5% noise on modal data. The results show a high level of accuracy of the proposed index for identifying the location of the damaged elements in beams.

1. Introduction

Maintenance of the structures to increase the structural performance and lifetime is of great importance in machine elements design industry. A great deal of research studies has been conducted to identify and detect damage location in structural systems. The engineering structures endure some unforeseen exter-

✉ Hessam Mirgolbabaei, e-mails: mirgolbabaei@gmail.com, hmirgolb@d.umn.edu

[1]Department of Civil Engineering, University of Mazandaran, Babolsar, Iran.

[2]Department of Mechanical and Industrial Engineering, University of Minnesota Duluth, Duluth, Minnesota, United States of America. ORCID: 0000-0002-2747-149X

nal loads during their lifetime; they are likely to be exposed to damages and catastrophic failure. To this end, structural health monitoring (SHM) has been an important field to study different methods for identification and localization of the structural damages. These methods can be classified into i) time domain, and ii) frequency domain approaches. The time-domain approach has been proposed to detect the damages based on changes in displacement, accelerations, or strains. The changes in natural frequency [1], mode shapes, power spectral density [2], or mode shape curvatures [3–6] are used as parameters for identification of damages in frequency-domain approaches. Most well-known methods are based on frequency and modal data, which are relatively easy to measure in real structures. Because of direct relationship between modal parameters (e.g., natural frequency and mode shape) and stiffness of the structures, any changes in the stiffness lead to changes in the modal frequencies and shapes. Fayyah et al. [7] proposed an index based on the combined effect of both natural frequencies and mode shapes when a change in stiffness of the structural element occurs for detecting the damage severity in structural elements. Their proposed index compared the factor of reduction in stiffness according to reduction in natural frequencies and the factor of reduction in stiffness according to the change in mode shape. Tomaszewska and Szafrański [8] focused on applicability of two modal identification techniques; peak picking based on correlation analysis for ambient vibrations and eigensystem realization algorithm formulated for free-decay vibrations investigation. The techniques were evaluated on masonry tower and steel railway bridge. Hasni et al. [9] conducted an artificial intelligence approach for the detection of distortion- induced fatigue cracking of steel bridge girders based on the data provided by self-powered wireless sensors. In their study, the sensors had series of memory gates that cumulatively recorded the duration of the applied strain. They characterized the output from the sensors by Gaussian cumulative density function. They concluded that their models had acceptable detection performance, specifically for cracks larger than 10 mm. Ciambella and Vestroni [10] studied the localization of stiffness variation in damaged beams through modal curvatures by applying a perturbative solution of the Euler–Bernoulli equation. Donskoy and Liu [11] proposed and investigated a baseline-free Vibro-Acoustic Modulation damage detection approach that does not require the monitoring of relative Modulation Index change. Farrar et al. [12] adopted a statistical approach in their process of vibration- based damage detection and applied it to a large-scale laboratory structure. They showed that changes in frequency would not yield any information about the location of damage, though they detect the presence of damage. Owolabi et al. [13] experimentally investigated damage detection in beams by measuring changes in the first three natural frequencies and the corresponding acceleration frequency response function. Fayyadh and Razak [14] proposed a new damage index based on a combination of mode shape vector and its derivatives. Efficiency of the index was examined by comparing it with COMAC for

trivial damages. Behera and et al. [15] identified the location and intensity of an inclined open edge crack in a cantilever beam using finite element method validated by experimental measurement. Their proposed method was based on measured frequencies and mode shapes of the beam. There has been another study conducted by Karimi et al. [16] that focused on free vibration analysis of damaged functionally graded beams based on the first-order shear deformation theory.

In the present research study, a new damage index is proposed based on mode shapes and their derivatives. One of the advantages of this new indicator is its applicability on beams to locate single and multiple structural damages. The numerical model was created based on finite element method which is programmed in MATLAB. To validate the model, its results are compared with those of an experimental test. The efficiency of the proposed index is examined in different boundary conditions using various numerical examples and comparing the results with those of some other indices. The paper is organized as follows: A summary of governing equations are presented. Then, the proposed damage index is introduced. In the next step, accuracy of the numerical modeling is validated through an experimental model. After that, the application and efficiency of the proposed index is evaluated using numerical examples. To demonstrate the accuracy of the proposed index in locating damaged elements, the results of the index are compared with those of some other indices. Finally, a summary of the results is presented.

2. Theory of the problem

2.1. Governing equations

Generally, the linear free vibration equation of an undamped system is expressed as:

$$[M]\{\ddot{x}\} + [K]\{x\} = 0, \tag{1}$$

where, $[M]$ is the mass matrix, $[K]$ is stiffness matrix, $\{x\}$ is the displacement vector, and $\{\ddot{x}\}$ is second derivative of the displacement vector. The solution of the differential equation can be generally written as $x = Ae^{rt}$, with r being a complex number expressed as $r = \pm iw$. Substituting x and its derivatives into the above equation leads to $([k] - w^2[M])\{x\} = 0$. In this equation, w represents the natural frequency. Eigenvalue and eigenvector matrix that are the natural frequencies, w, and mode shapes, $\{\varphi\}$, respectively, are built by performing the eigenvalue decomposition of this equation.

2.1.1. Beam element formulation

As shown above, the stiffness and mass matrices of a structure are used for finding the modal data. The stiffness and mass matrices of the beam element in

a finite element model, by considering the transverse displacement and rotation as the two degrees of freedom (Fig. 1) in each node, are as follows [17]:

$$[k] = \frac{EI}{L^3}\begin{bmatrix} 12 & 6L & -12 & 6L \\ 6L & 4L^2 & -6L & 2L^2 \\ -12 & -6L & 12 & -6L \\ 6L & 2L^2 & -6L & 4L^2 \end{bmatrix}, \tag{2}$$

$$[M] = \frac{\rho AL}{420}\begin{bmatrix} 156 & 22L & 54 & -13L \\ 22L & 4L^2 & 13L & -3L^2 \\ 54 & 13L & 156 & -22L \\ -13L & -3L^2 & -22L & 4L^2 \end{bmatrix}, \tag{3}$$

where, E, I, L, and ρ are the modulus of elasticity, the moment of inertia, the length, and the mass density of the beam, respectively.

It is noteworthy that, by "height", the authors mean the "thickness".

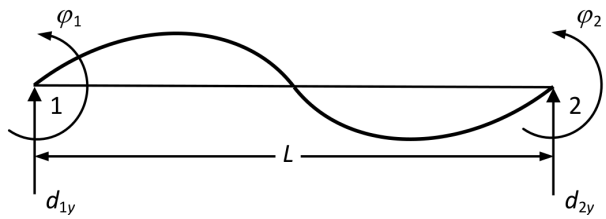

Fig. 1. Demonstration of the degrees of freedom for beam element and positive sign convention based on FEM method

2.2. Proposed damage index

In this study, to detect the damages in the structure, a new index called Damage Localization Index (*DLI*) based on mode shape and its derivatives has been proposed as follows:

$$DLI_{(i)} = \frac{\sum_{n=1}^{nm}\left\{\left|\left(\left|\left(\varphi_{h(i.n)} \times \left|\varphi''_{d(i.n)}\right|\right)\right| - \left|\left(\varphi_{d(i.n)} \times \left|\varphi''_{h(i.n)}\right|\right)\right|\right)\right\} \times \varphi''_{dh(i.n)}}{nm}, \tag{4}$$

$$\varphi''_{dh(i.n)} = \left\{\left|\varphi''_{d(i.n)}\right| - \left|\varphi''_{h(i.n)}\right|\right\}, \tag{5}$$

where nm is the number of modes considered, n denotes the number of nodes, $\varphi''_{h(i.n)}$ and $\varphi''_{d(i.n)}$ are mode shapes of the undamaged and damaged beams at n-th mode in the i-th degree of freedom (*dof*) respectively, and $\varphi''_{h(i.n)}$ and $\varphi''_{d(i.n)}$ are

the curvature mode shapes of the undamaged and damaged beams at n-th mode in i-th *dof*, respectively [18].

Curvature mode shape ($\varphi''_{i.n}$) would be obtained by using a central difference approximation as follows:

$$\varphi''_{i.n} = \frac{\varphi_{i-1.n} - 2\varphi_{i.n} + \varphi_{i+1.n}}{h^2}, \tag{6}$$

where: $\varphi_{i.n}$ – mode shape at n-th mode in i-th *dof*, $\varphi''_{i.n}$ – curvature mode shape at n-th mode in i-th *dof*, h – length of element.

For a better presentation of the proposed index values, the *DLI* is normalized in each node of structure, considering the mean and standard deviation. Also, negative values have been replaced with zero.

2.3. Validation of the numerical model

2.3.1. Beam

To verify the applied model, an undamaged cantilever beam which has been examined by Behera et al. [15] is studied in this section. Length, width, and height (i.e., thickness) of the beam are 800 mm, 60 mm, and 6 mm, respectively. The modulus of elasticity, the material density, and Poisson's ratio are $7 \cdot 10^{10}$ N/m^2, 2710 Kg/m^3, and 0.346, respectively.

The first three natural frequencies resulted from the undamaged numerical and experimental models are compared in Table 1. Also, comparisons of the three mode shapes are displayed in Fig. 2.

Table 1.
Comparison between the calculated natural frequencies of the undamaged beam from the FE model and the measured ones from experimental model [15] for first three mode shapes

Results	First natural frequency	Second natural frequency	Third natural frequency
Numerical model	7.696	48.732	135.095
Experimental model [15]	8.217	50.256	141.13
Error (%)	4.12%	4.81%	4.47%

The comparison, as demonstrated in Table 1, reveals that the natural frequencies and mode shapes obtained from the numerical model and the experimental measurements [15] are in ideal agreement. That confirms the accuracy of the present numerical model.

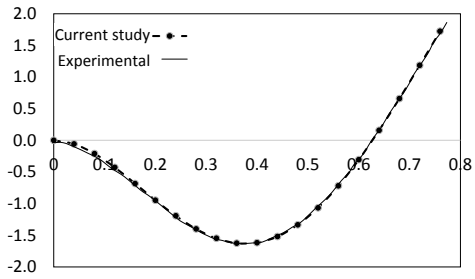

(a) first mode

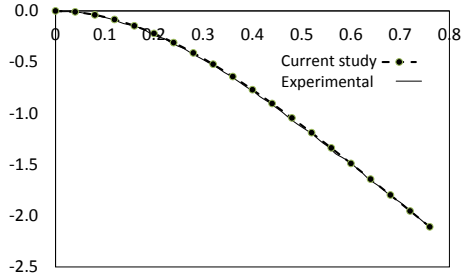

(b) second mode

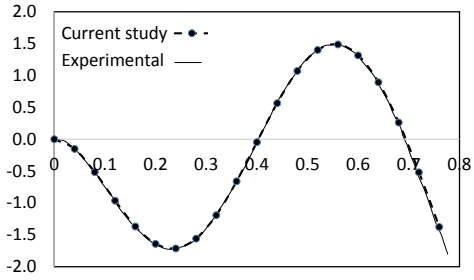

(c) third mode

Fig. 2. Mode shapes for numerical model and experimental test [15]

3. Numerical examples

3.1. Numerical model

In this section, to assess the applicability of the proposed index, different numerical examples are presented. A beam with different supporting conditions and damage scenarios is considered. Characteristics of the studied beam are presented in Table 2.

Table 2.

The properties of the numerical modeled beam

Density (ρ)	7850 Kg/m^3
Elasticity modulus (E)	200 GPa
Poisson's ratio (ν)	0.3
Moment of Inertia (I)	$1.953 \cdot 10^{-4}$ m^4
Area (A)	0.375 m^2
Length (L)	1 m

To better evaluate the proposed index, the obtained results are compared with two indicators, MSEBI [19] that is shown in Eq. (7) through (11), and CDF [20] that is defined in Eq. (12), as follows:

$$MSEBI^e = \max\left[0,\ \frac{mnmse^{e^d} - mnmse^{e^h}}{mnmse^{e^h}}\right], \tag{7}$$

$$mse_i^e = \frac{1}{2}\varphi_i^{eT} K_e \varphi_i^e, \quad i = 1, \ldots, ndf, \quad e = 1, \ldots, nte, \tag{8}$$

$$mse_i = \sum_{e=1}^{nte} nmse_i^e, \quad i = 1, \ldots, ndf, \quad e = 1, \ldots, nte, \tag{9}$$

$$nmse_i^e = \frac{mse_i^e}{mse_i}, \tag{10}$$

$$mnmse^e = \frac{\sum_{n=1}^{nm} nmse_i^e}{nm}, \tag{11}$$

$$CDF = \frac{1}{nm}\sum_{n=1}^{nm}\left(\varphi''_{hi} - \varphi''_{di}\right)_n . \tag{12}$$

In the above equations, nm is the number of modes considered. The nte and ndf are element numbers and the total degrees of freedom of the structure, respectively. mse_i^e and $nmse_i^e$ are the modal strain energy of the e-th element in i-th mode and the normalized MSE, respectively. $mnmse^e$ is the mean of the normalized MSE. φ''_{hi} and φ''_{di} are the mode shape curvature of undamaged and damaged structures, respectively.

Dimensions and finite element model of the beam are illustrated in Fig. 3. It should be noted that the mesh sizes are selected in such a way that decreasing

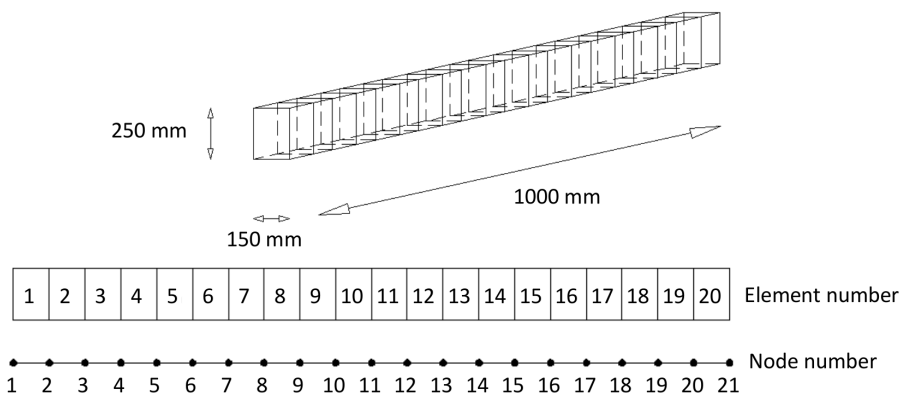

Fig. 3. Finite element modeling of the beam

these sizes does not have any special effect on results. In other word, the grid independency analysis has been performed, and the values reported in this study are from the models with no grid size sensitivity.

3.2. Simply supported beam

The first example studied here is a beam with two simply supported ends at nodes 1 and 21, as shown in Fig. 3. Different damage scenarios are considered as defined in Table 3. Damages in elements are simulated for different modulus of elasticity, E. According to Eq. (2), the stiffness of the structural elements, K, and the bending stiffness, EI, are linearly correlated. Reducing either the modulus of elasticity or the moment of inertia is equivalent to reducing the reduction in stiffness of the beam. If, for instance, 20% reduction in the thickness of the element is considered as a damage, the moment of inertia will reduce to $(1-0.2)^3 = 0.512$ of its initial value i.e., about 50% reduction in moment of inertia of the cross section of the beam happens. In other word, the modulus of elasticity can be multiplied by this coefficient (0.512), which leads to the same EI, thus K reduction. However, reduction in the modulus of elasticity results in the same reduction of the K value. That means the modulus of elasticity can be manipulated to account for the thickness reduction, accordingly. For instance, a 20% reduction in stiffness K, that is modeled by 20% reduction in E, is equivalent to having the beam section with $\sqrt[3]{(1-0.2)} = 92.8\%$ of its original thickness.

Table 3.

Damage scenarios

Damage scenarios	Element number	Reduction in elasticity modulus of the element(s)
Damage-1	5, 10	10%, 20%
Damage-2	2, 20	20%, 10%
Damage-3	6, 12, 17	15%, 5%, 10%

The proposed damage index (DLI) is applied to the abovementioned scenarios and the results are presented in Fig. 4. During the damage detection process for all the three scenarios, only the first flexural mode is applied and no noise in the modal data is considered.

For "damage-1" scenario, the damaged elements are introduced in quarter-span and mid-span. For "damage-2" scenario, the damaged element is located adjacent to the support. For "damage-3" scenario, multiple damages are investigated. In the following, the results of the calculation of DLI, MSEBI and CDF are presented for the different damage scenarios defined in Table 3. To better compare and evaluate the cases, maximum absolute values of indicators – DLI, are set to unity. Additionally, the number of modes for different scenarios are similar. To eliminate, or at least decrease, any false detections, values of indicator – DLI, less than 0.05 are ignored.

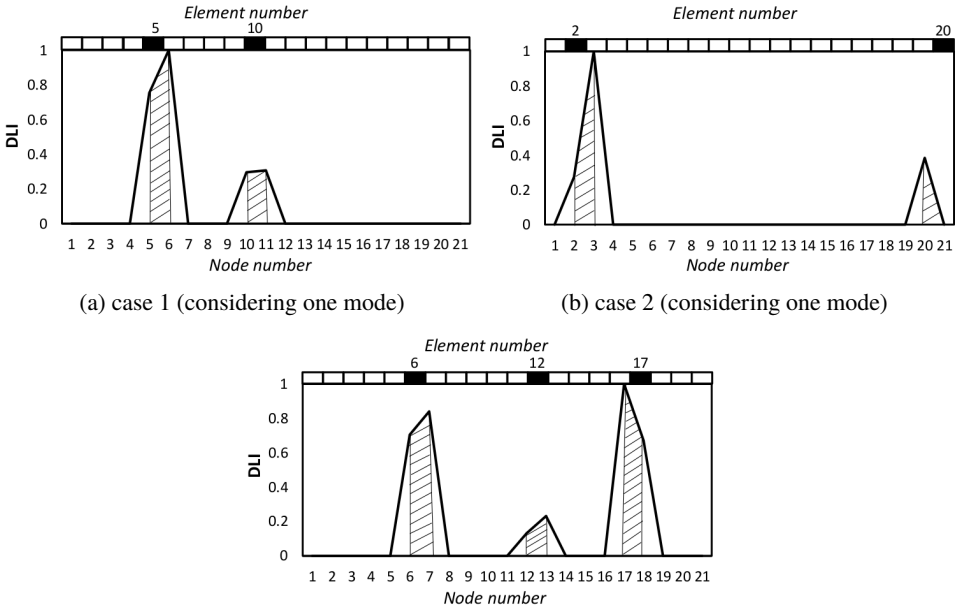

(a) case 1 (considering one mode)

(b) case 2 (considering one mode)

(c) case 3 (considering one mode)

Fig. 4. The results of damage detection based on DLI index in simply supported beam for noise free condition

Fig. 5 demonstrates the comparison between DLI, CDF, and MSEBI values for different damage scenarios. “Damage-1” is clearly and exactly identified by DLI and CDF, while incorrect detections occurs at undamaged location (element no. 7, 15, 19) using MSEBI. Accurate detection is also conducted for “damage-2” and “damage-3”, by both DLI and CDF. However, “damage-2” and “damage-3” are missed by MSEBI. Furthermore, MSEBI results show that damages occur at intact elements (for “damage-2”, element no. 12 and 15, and for “damage-3”, element no. 17).

In conclusion, the proposed index accurately performed damage detection at different locations, even near the support. It can be deduced that CDF has also localized damage with proper precision. However, MSEBI has errors in the diagnosis of damaged elements. Additionally, for evaluating the sensitivity of damage localization against the noise-polluted modal information, the noisy signals are generated at a rate of 3% and 5%. Considering 3% noise, for “damage-1”, “damage-2”, and “damage-3”, it was clearly found that significant values of DLI appeared in damaged elements, as shown in Fig. 6. MSEBI has not identified damaged element (element no. 5) for “damage-1”. For instance, as demonstrated in Fig. 6a, the element no. 5 and element no. 10 (embedded in between node no. 5 and 6) are supposed to be the damaged elements. The DLI accurately inspects the node no. 5 and node no. 11 as the damage locations. Therefore, detections are exact location detection, corresponding to the damage locations, elements 5

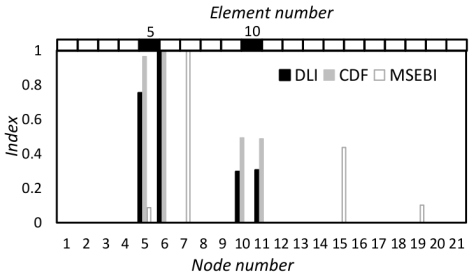

(a) case 1 (considering one mode)

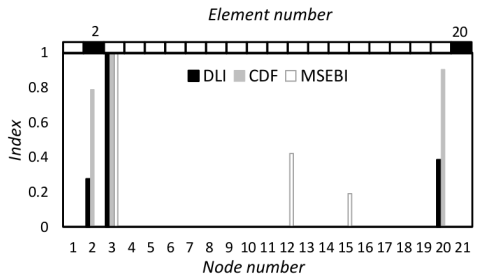

(b) case 2 (considering one mode)

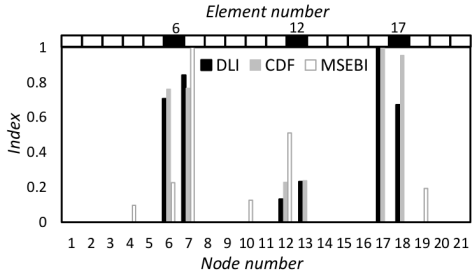

(c) case 3 (considering one mode)

Fig. 5. Comparison of the results of damage detection based on DLI, MSEBI and CDF indices in simply supported beam for noise free condition

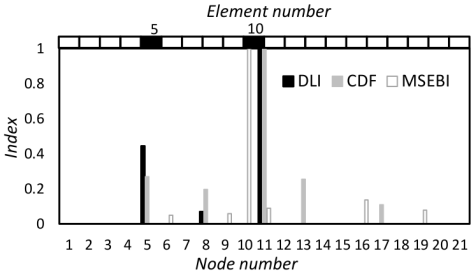

(a) case 1 (considering one mode)

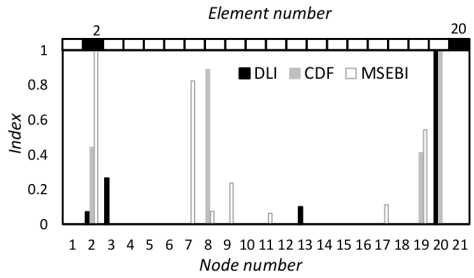

(b) case 2 (considering one mode)

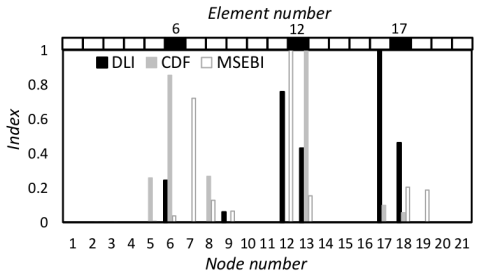

(c) case 3 (considering one mode)

Fig. 6. Comparison of the results of damage location detection for DLI, MSEBI and CDF indices in simply supported beam, considering 3% noise

and 10. As can be seen from Fig. 6a, CDF also accurately detects node 5 (left-hand side of element 5) and nodes 10 and 11 (the left-hand side and right-hand side nodes of element no. 10). However, MSEBI does not detect the damage element 5 with a significant value at node 6, compared to those of DLI and CDF at node 5. In a similar fashion, node 11 is detected by only a relatively small MSEBI value.

Fig. 6b demonstrates the inefficiency of MSEBI and CDF detecting healthy elements (nodes), while representing a descent detection by DLI. Fig. 6c demonstrates a decent detection of the damaged elements (corresponding nodes) by all three indicators, at the first two damages. However, CDF detects a healthy element (nodes 5 and 8) with relatively significant values.

Overall, the proposed index performed better in detecting damage than the other two indicators, especially at the boundaries.

In the following, considering 5% noise, the proposed index performance is evaluated in higher noise conditions.

The results of DLI are compared to two indicators CDF and MSEBI, considering 5% noise, and are demonstrated in Fig. 7. Like the previously obtained results, and despite 5% noise, damage localization by DLI is acceptable. Comparison of the results shows that the DLI can accurately locate the damage in both noise free and noisy conditions.

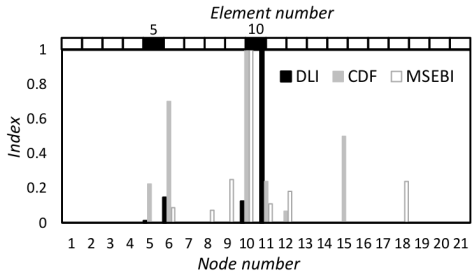

(a) case 1 (considering one mode)

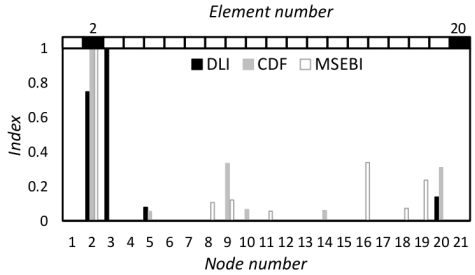

(b) case 2 (considering five modes)

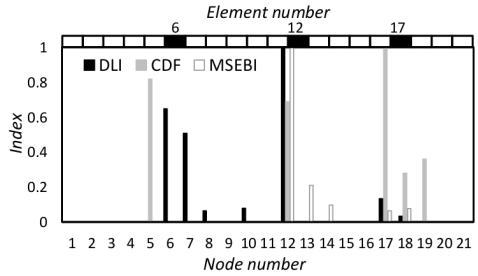

(c) case 3 (considering five modes)

Fig. 7. Comparison of the results of damage location detection for DLI, MSEBI and CDF indices in simply supported beam, considering 5% noise

3.3. Fixed-end beam

In this section, a fixed boundary of the damaged beam with the same parameters as the simply supported beam is studied. It means that in nodes 1 and 21, there is no rotation and transverse motion. Damage scenarios are defined in Table 4.

Table 4.

Damage scenarios of the fixed end beam

Damage scenarios	Element number	Reduction in elasticity modulus of the element(s)
Damage-1	7, 12	15%, 10%
Damage-2	5, 6, 13	5%, 10%, 15%

Fig. 8 demonstrates the damage location detection results in the fixed end beam for "damage-1" and "damage-2". Considering the two adjacent damaged elements in second scenario, the capability of the proposed index is investigated. Fig. 8 shows that the damaged elements are correctly localized by DLI.

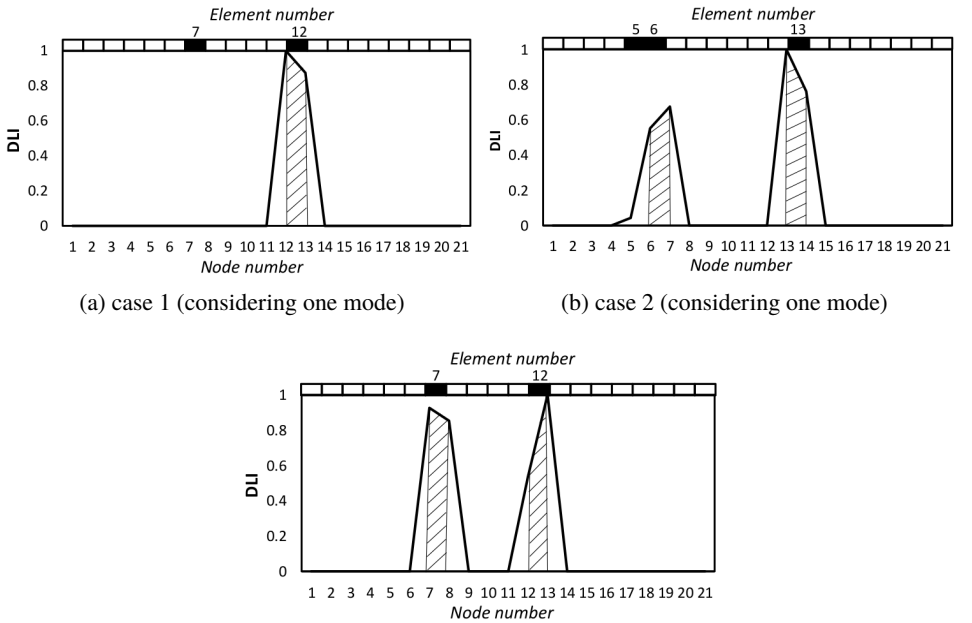

(a) case 1 (considering one mode)

(b) case 2 (considering one mode)

(c) case 1 (considering two modes)

Fig. 8. The results of damage locating for DLI index in fixed end beam for noise free condition

DLI, MSEBI, and CDF are calculated and compared for two damage cases as listed in Table 4, in Fig. 9. As previously mentioned, for better comparison,

maximum absolute values of DLI indicators that equals to 1 and the same number of modes are used in their calculations. Also, DLI values that are less than 0.05 are set to zero.

"Damage-1" is clearly identified using the first two modes, as shown in Fig. 9a.

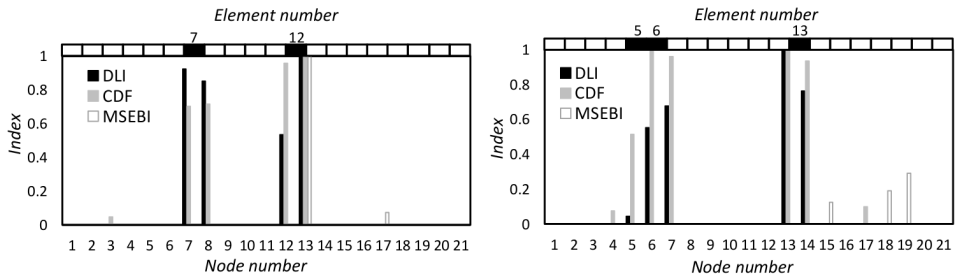

(a) case 1 (considering one mode) (b) case 2 (considering two modes)

Fig. 9. Comparison of the results of damage locating for DLI, MSEBI and CDF indices in fixed end beam for noise free condition

"Damage-1" and "damage-2" were located with high accuracy by DLI and CDF indicators. However, MSEBI is not able to identify the damaged element (for "damage-1", element no. 7, and for "damage-2", all damaged elements).

A comparison of the results obtained from calculations shows that DLI and CDF indicators more accurately predict the damage locations than MSEBI index. To have a better comprehension of the DLI capability, 3% and 5% noise was added to the calculated mode shapes. Fig. 10 and Fig. 11 represent the comparisons between the results from DLI, CDF, and MSEBI referenced in literature.

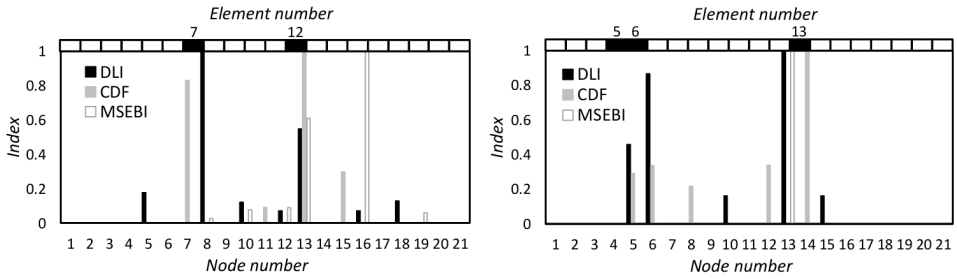

(a) case 1 (considering two modes) (b) case 2 (considering one mode)

Fig. 10. Comparison of the results of damage locating for DLI, MSEBI and CDF indices in fixed end beam for 3% noise condition

The DLI represents more reliable results compared to the other two indicators, CDF and MSEBI, in the presence of noise, as shown in Fig. 10 and Fig. 11.

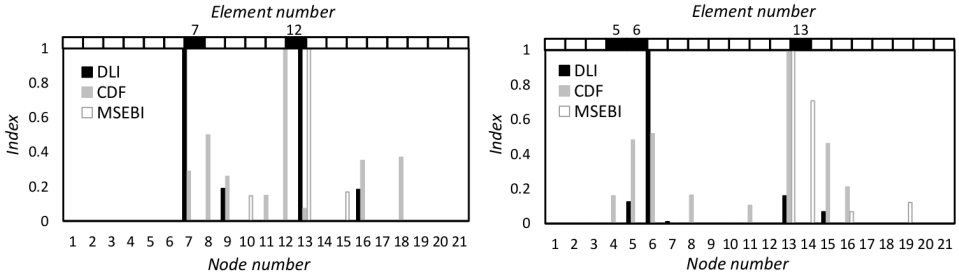

(a) case 1 (considering two modes) (b) case 2 (considering one mode)

Fig. 11. Comparison of the results of damage locating for DLI, MSEBI and CDF indices in fixed end beam for 5% noise condition

3.4. Cantilever beam

In this part, a cantilever beam is studied as another numerical example. Rotation and transverse motion are restricted on node 1. For the cantilever, the same properties of the beam described in section 2.3, such as damage type and number of elements, are used in this section. The proposed index values are investigated for three different states: noise-free, 3% noise, 5% noise. Three different damage scenarios are presented in Table 5. To evaluate the accuracy of the proposed indexes, damage detection is tested on two adjacent damaged elements, for the damage type "damage-1". By determining one of the end elements (free end of the beam) for "damage-2", the ability of the proposed index is measured in this case, as well. For "damage-3", the damage was created in the boundary element (element no. 20).

Table 5.

Damage scenarios of the cantilever beam

Damage scenarios	Element number	Reduction in elasticity modulus of the element(s)
Damage-1	4, 5, 13	10%, 15%, 5%
Damage-2	19	10%
Damage-3	20	15%

As demonstrated in Fig. 12, to increase the accuracy of locating the damaged element, 3 mode shapes are needed for "damage-1" while only 1 mode shape is considered for "damage-2". For accurately detecting the location of the damage, 4 mode shapes must be considered for "damage-3", because of the boundary element used as the damaged element. As shown in Fig. 12c, the highest value of the DLI is measured in element 20. Applying on the boundary element, some detections also occurred at undamaged points. The performance of DLI in comparison against MSEBI and CDF is demonstrated in Fig. 12. It is obvious that the proposed index – DLI, performs better than the other two indicators, as shown in Fig. 13c.

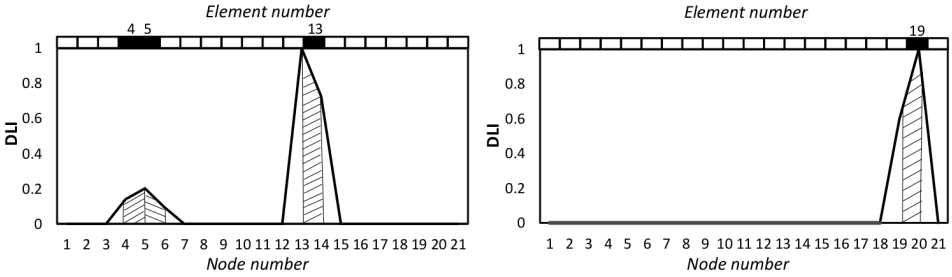

(a) case 1 (considering two modes) (b) case 2 (considering one mode)

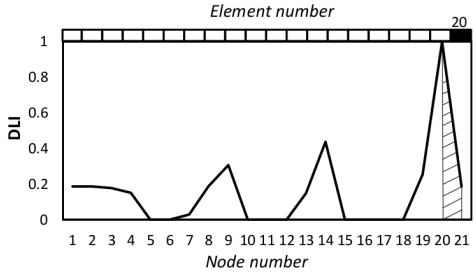

(c) case 3 (considering four modes)

Fig. 12. Comparison of the results of damage detection in the cantilever beam from DLI, for noise free conditions

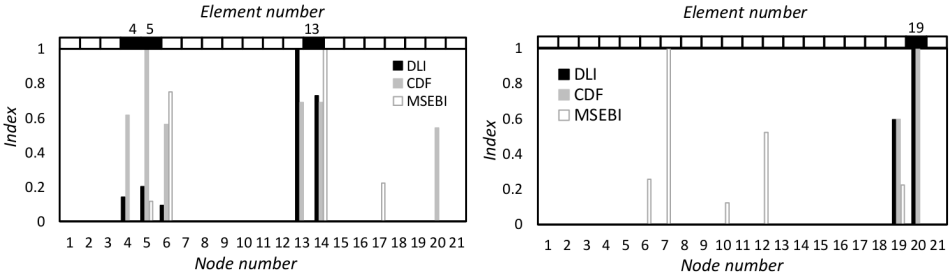

(a) case 1 (considering two modes) (b) case 2 (considering one mode)

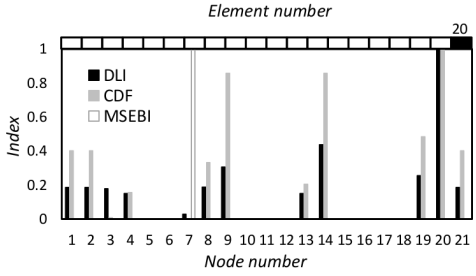

(c) case 3 (considering four modes)

Fig. 13. Comparison of the results of damage detection based on DLI, MSEBI, and CDF indices in cantilever beam for noise free conditions

Due to unavoidable use of forward (or backward) finite difference at the boundaries, the precision of detecting methods is often reduced in these areas. An important advantage of the proposed index is the proper diagnosis of the damaged elements at the boundaries (as shown for "damage-3").

As shown in Fig. 13a, damaged elements 4, 5, and 13 are correctly detected by DLI whereas CDF incorrectly detected element 20 as the damaged element. Additionally, MSEBI does not detect the damaged element 4. To make more accurate detection, two first bending modes are used for "damage-1". For "damage-2", DLI and CDF identifies element no. 19 with high accuracy, whereas an acceptable accuracy is not observed from MSEBI values. For "damage-3", as shown in Fig. 13c, DLI and CDF can detect damaged location by displaying the maximum value in the damaged element – element no. 20, while the maximum value of MSEBI is indicated in an intact element.

In the following, the measurement noise is incorporated by 3% and 5% error values for mode shapes. The results of the comparison between three indicators are shown in Fig. 14 and Fig. 15.

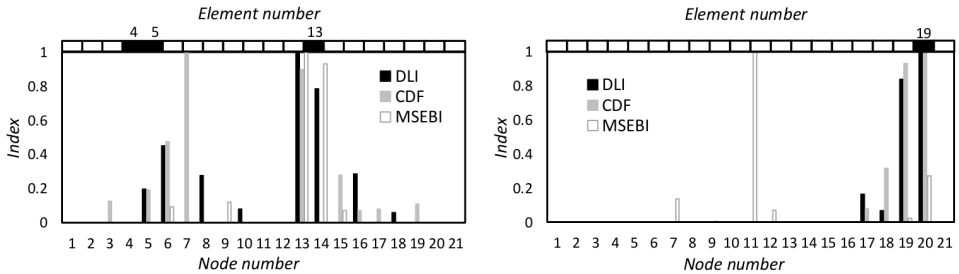

(a) case 1 (considering two modes)

(b) case 2 (considering one mode)

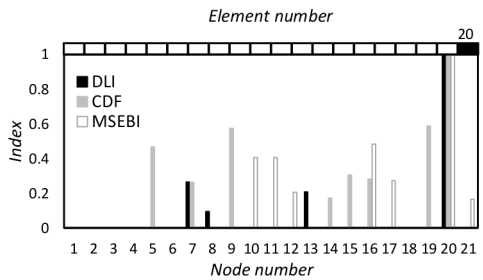

(c) case 3 (considering four mode)

Fig. 14. Comparison of the results of damage detection based on DLI, MSEBI, and CDF indices in cantilever beam for 3% noise condition

Figs. 14 and 15 show the results in which the effect of measurement noise on the performance of the proposed index and two other indicators is considered. The results reveal that the proposed index is more precise than the other two indicators

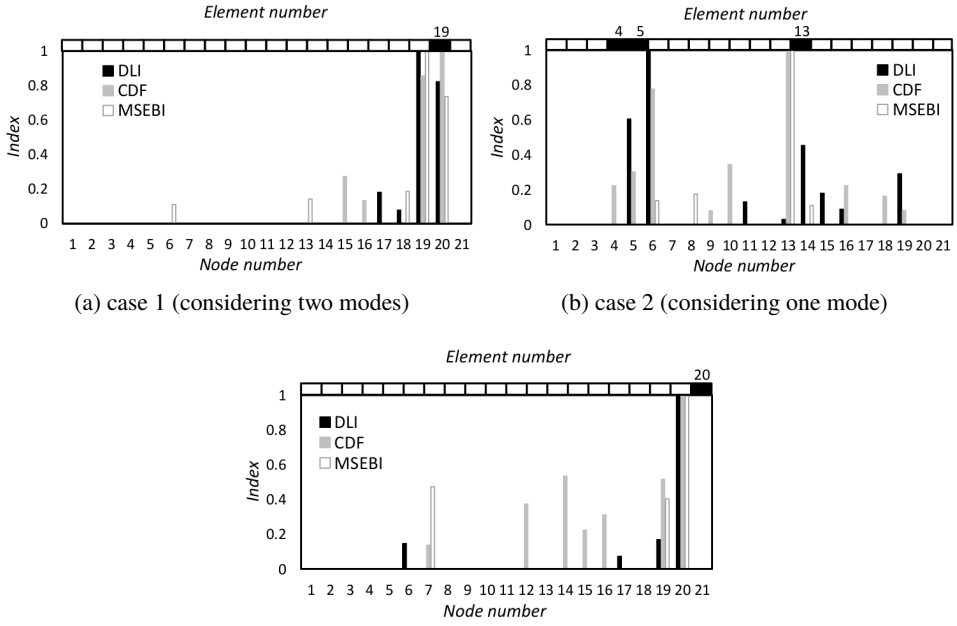

(a) case 1 (considering two modes)

(b) case 2 (considering one mode)

(c) case 3 (considering four mode)

Fig. 15. Comparison of the results of damage detection for DLI, MSEBI and CDF indices in cantilever beam for 5% noise condition

(CDF and MSEBI) under noisy condition. It also provides more accurate identifying than free noisy state in three scenarios. In conclusion, the proposed index can be considered as an effective indicator for cantilever beams.

4. Conclusion

The purpose of the present work is the detection of the presence and location of damage(s) in beam structure. Regardless of the type of the damage, any form of damage in the beam can be represented by reduction of the stiffness value of the beam at that section(s), thus the stiffness value of the whole beam structures. To this end, the decrease in the stiffness of the beam is how the damage detection is performed in this study. The decrement of the stiffness is incorporated as the decrement of the modulus of elasticity in the analytical part of the present study. However, the type of the damage can be in the form of reduction of the thickness of the element(s) of the beam. The stiffness of the beam is related to EI, thus Et^3, with E and t being the modulus of elasticity and the thickness of the beam section, respectively. As a result, thickness reduction can be easily represented by a decrease in E, instead. As an example, corrosion in a beam section(s) can be represented by corresponding decrease of the second moment of inertia, thus decrease of the stiffness that can also be simulated by a corresponding change in

the beam's modulus of elasticity. In general, the damages in structures differs per the application of them, and thus can be caused by different circumstances such as external load, interactions with other parts of the structure, fatigue, thermal effects, humidity, etc. However, all those circumstances can be interpreted as a change of the stiffness of the element(s) of the beam thus modulus of elasticity of the structure.

In the present study, a new index called "DLI" is introduced for the purpose of damage location detection in beams. To validate the numerical modeling of the beam, the experimental models are used, and the first three frequencies obtained from the numerical study are validated against the experimental data. The comparison proved the accuracy of the numerical model. The beams with three different supporting conditions and various damage scenarios are then studied. The obtained results demonstrate the robustness of the proposed indicator, DLI, to locate both single and multiple damages at different locations including the mid-elements, elements near the supporting, and adjacent elements. The results showed that in most cases, the proposed index can identify the correct location of the damage in the beam, using only one shape mode. Damage detection by the DLI is also assessed in minor damaged areas and the efficiency of detection is verified. To investigate the performance of the proposed index, a comparison is made between DLI and two other well-known indices reported in the literature - MSEBI and CDF. The results show that the proposed index performs better than the other two indicators in locating the damages. Additionally, noise-sensitivity of the proposed index is studied. The results demonstrate that DLI is more effective than MSEBI and CDF in detecting the damage locations. Overall, based on the obtained results, it can be concluded that the proposed index can identify the damage locations in real engineering structures, with reasonable accuracy. It is always desired to detect the damage(s) in the beam with considering a smaller number of shape modes, as the implementation will be easier in practice. However, the greater number of damages present in the beam, or larger the noise in the information obtained from the beam, the larger the number of shape modes required to perform the detection. For the sake of demonstration of this point, a variety of examples in this article are presented. As can be deduced from the results, in most circumstances, the proposed method can precisely detect the damage location with least number of modes, in comparison to other methods proposed in literatures.

Manuscript received by Editorial Board, May 22, 2021;
final version, August 11, 2021.

References

[1] M. Dilena, M.F. Dell'Oste, and A. Morassi. Detecting cracks in pipes filled with fluid from changes in natural frequencies. *Mechanical Systems and Signal Processing*, 25(8):3186–3197, 2011. doi: 10.1016/j.ymssp.2011.04.013.

[2] J.M. Dulieu-Barton, W.J. Staszewski, and K. Worden. *Structural Damage Assessment Using Advanced Signal Processing Procedures: Proceedings of the International Conference on Damage Assessment of Structures (DAMAS '97)*. Sheffield, England, 30 June - 2 July, 1997, Sheffield Academic Press, 1997,

[3] W. Xu, M. Cao, W. Ostachowicz, M. Radzieński, and N. Xia. Two-dimensional curvature mode shape method based on wavelets and Teager energy for damage detection in plates. *Journal of Sound and Vibration*, 347:266–278, 2015. doi: 10.1016/j.jsv.2015.02.038.

[4] D.V. Jauregui and C.R. Farrar. Damage identification algorithms applied to numerical modal data from a bridge. In: *14th International Modal Analysis Conference*, Dearborn, USA, 12-15 February, 1996.

[5] N. Navabian, M. Bozorgnasab, R. Taghipour, and O. Yazdanpanah. Damage identification in plate-like structure using mode shape derivatives. *Archive of Applied Mechanics*, 86:819–830, 2016. doi: 10.1007/s00419-015-1064-x.

[6] N. Navabian, R. Taghipour, M. Bozorgnasab, and J. Ghasemi. Damage evaluation in plates using modal data and firefly optimisation algorithm. *International Journal of Structural Engineering*, 9(1):50-69, 2018. doi: 10.1504/IJSTRUCTE.2018.090750.

[7] M.M. Fayyadh, H.A. Razak, and Z. Ismail. Combined modal parameters-based index for damage identification in a beamlike structure: theoretical development and verification. *Archives of Civil and Mechanical Engineering*, 11(3):587–609, 2011. doi: 10.1016/S1644-9665(12)60103-4.

[8] A. Tomaszewska and M. Szafrański. Study on applicability of two modal identification techniques in irrelevant cases. *Archives of Civil and Mechanical Engineering*, 20:13, 2020. doi: 10.1007/s43452-020-0014-8.

[9] H. Hasni, A.H. Alavi, P. Jiao, and N. Lajnef. Detection of fatigue cracking in steel bridge girders: A support vector machine approach. *Archives of Civil and Mechanical Engineering*, 17(3):609–622, 2017. doi: 10.1016/j.acme.2016.11.005.

[10] J. Ciambella and F. Vestroni. The use of modal curvatures for damage localization in beam-type structures. *Journal of Sound and Vibration*, 340:126–137, 2015. doi: 10.1016/j.jsv.2014.11.037.

[11] D. Donskoy and D. Liu. Vibro-acoustic modulation baseline-free non-destructive testing. *Journal of Sound and Vibration*, 492:115808, 2021. doi: 10.1016/j.jsv.2020.115808.

[12] C.R. Farrar, S.W. Doebling, and D.A. Nix. Vibration–based structural damage identification. *Philosophical Transactions of the Royal Society A. Mathematical, Physical and Engineering Sciences*, 359(1778):131–149, 2001. doi: 10.1098/rsta.2000.0717.

[13] G.M. Owolabi, A.S.J. Swamidas, and R. Seshadri. Crack detection in beams using changes in frequencies and amplitudes of frequency response functions. *Journal of Sound and Vibration*, 265(1):1–22, 2003. doi: 10.1016/S0022-460X(02)01264-6.

[14] M.M. Fayyadh and H.A. Razak. Weighting method for modal parameter based damage detection algorithms. *International Journal of Physical Sciences*, 6(20):4816–4825, 2011.

[15] R.K. Behera, A. Pandey, and D.R. Parhi. Numerical and experimental verification of a method for prognosis of inclined edge crack in cantilever beam based on synthesis of mode shapes. *Procedia Technology*, 14:67–74, 2014. doi: 10.1016/j.protcy.2014.08.010.

[16] S. Karimi, M. Bozorgnasab, R. Taghipour, and M. M. Alipour. A novel spring-based model for damage investigation of functionally graded beams. *Journal of Solid Mechanics*, 2021 (in print).

[17] S.S. Rao. *The Finite Element Method in Engineering*, 6th edition. Butterworth-Heinemann, 2018.

[18] A.K. Pandey, M. Biswas, and M.M. Samman. Damage detection from changes in curvature mode shapes. *Journal of Sound and Vibration*, 145(2):321–332, 1991. doi: 10.1016/0022-460X(91)90595-B.

[19] S.M. Seyedpoor. A two stage method for structural damage detection using a modal strain energy based index and particle swarm optimization. *International Journal of Non-Linear Mechanics*, 47(1):1–8, 2012. doi: 10.1016/j.ijnonlinmec.2011.07.011.

[20] M.M.A. Wahab and G. De Roeck. Damage detection in bridges using modal curvatures: application to a real damage scenario. *Journal of Sound and Vibration*, 226(2):217–235, 1999. doi: 10.1006/jsvi.1999.2295.

[21] A. Esfandiari, F. Bakhtiari-Nejad, and A. Rahai. Theoretical and experimental structural damage diagnosis method using natural frequencies through an improved sensitivity equation. *International Journal of Mechanical Sciences*, 70:79–89, 2013. doi: 10.1016/j.ijmecsci.2013.02.006.